PROCEEDINGS OF SPIE

SPIEDigitalLibrary.org/conference-proceedings-of-spie

Height-modulation of diffraction gratings by light-controlled capillary force lithography for structural coloring

Myung Gi Ji, Jaeyoun Kim

Myung Gi Ji, Jaeyoun Kim, "Height-modulation of diffraction gratings by light-controlled capillary force lithography for structural coloring," Proc. SPIE 12434, MOEMS and Miniaturized Systems XXII, 1243402 (15 March 2023); doi: 10.1117/12.2650950

SPIE.

Event: SPIE OPTO, 2023, San Francisco, California, United States

Height-Modulation of Diffraction Gratings by Light-Controlled Capillary Force Lithography for Structural Coloring

Myung Gi Ji[a] and Jaeyoun Kim[a*]
[a]Department of Electrical and Computer Engineering, Iowa State University of Science and Technology, Ames, IA USA 50011

ABSTRACT

Diffraction gratings are ubiquitous in many optical applications such as sensors, filters, and optical security devices. Capillary force lithography, which utilizes the capillary rise of photopolymer into nanoscale cavities, is a simple and rapid method to construct diffraction gratings without necessitating expensive instruments or complex steps. With the help of spatial light modulators, such as the digital micromirror device, the height of the grating can also be spatially modulated, printing spatially height-modulated gratings. When white light normally impinges on the grating, the light propagates into the grating interferes with light that propagates into air. By varying the height of the grating, the optical path lengths of two lights can be varied, leading to different interference effects and structural coloring. Judicious design of the grating's parameters and patterning process will even allow encoding of multiple images. In this work, by tuning the height of the grating through the light-controlled capillary force lithography, we demonstrate grating-based structural color printing. This technique is promising for producing the custom patterns for anti-counterfeiting, authentication, and cryptography.

Keywords: Nanotexture, Diffraction Grating, Capillary Force Lithography, Spatial Light Modulation, Digital Micromirror Device, Structural Color

1. INTRODUCTION

A nanotexture is a collection of nanopixels which take the form of nanopillars[1], nanolens arrays[2], and nanogratings[3]. Recently, the functionalities of the nanopixels have been enhanced by modulating their dimensions[4,5]. For example, randomly modulated depth and diameter of nanohole arrays on lens can enhance their anti-reflection[4]. Siddique et al. realized the random-height nanopillar arrays which can expand the range of glare suppression over a wide range of incidence angle and polarization[5].

The nanotexture with the pre-designed dimensions such as height, periodicity, and angle of incidence can produce the different optical characteristics[1–3]. The height of the nanotexture needs to be precisely adjusted at the nanoscale as a function of positions in order to actualize and improve their capabilities. Existing techniques such as scanning beam lithography[6], Shrinkage and swelling of the polymeric material[7], and grayscale lithography[8] can control the height as a function of position. However, they often necessitate a complex and costly fabrication step.

Here, we demonstrate the light controlled capillary force lithography (CFL) with spatial light modulator (SLM)[1] for the structural coloring of the diffraction gratings. In conventional CFL[9,10], the lack of controllability in nanocapillary actions to vary the nano pixel's height hindered from the wide utilization for many applications. In contrast to the conventional CFL, our new technique, which applying the optical premodification of the photopolymer's characteristics resulting from the dependence on the applied UV dose, is highly capable of controlling the height of the diffraction gratings as a function of position which in turn determines structural color. The proposed technique will provide a facile way to broaden the nanoscale manufacturing.

MOEMS and Miniaturized Systems XXII, edited by Hans Zappe, Wibool Piyawattanametha, Yong-Hwa Park, Proc. of SPIE Vol. 12434, 1243402 · © 2023 SPIE
0277-786X · doi: 10.1117/12.2650950

2. LIGHT-CONTROLLED CAPILLARY FORCE LITHOGRAPHY

2.1 Light-controlled capillary force lithography (CFL)

Figure 1 describes the process of light-controlled CFL technique schematically. It is very similar to the conventional CFL process except for the additional spatially modulated UV irradiation process (Figure 1e). By applying the spatially varying UV irradiation, the height of the nanotexture can be modulated as a function of position.

Firstly, a master mold was prepared with two photon polymerization lithography (TPL). To fabricate the master mold, IP-Dip2, ultraviolet (UV) curable photopolymer, was dropped on a fused silica substrate, followed by transferring to a Nanoscribe GmbH Photonic Professional GT2 system for patterning the structure using laser power of 20 mW and a laser scan speed of 10000 μm/s (Figure 1a). After the completion of the patterning process, the substrate was immersed in propylene glycol monomethyl ether acetate (PGMEA) solution for 5 min to remove the uncured photopolymer. Then, the substrate was subsequently immersed in the isopropyl alcohol for 5 min. Finally, the substrate was dried in ambient air condition (Figure 1b).

Secondly, as shown in the Figure 1c, the fabricated master mold (3 μm in pitch, 1.2 μm in height, 1.5 μm in width) was replicated with the poly(dimethylsiloxane) (PDMS) (Dow Corning Sylgard 184, 10 (base):1 (curing agent) weight ratio). After being cured for 10 hours at 70 °C, the PDMS replica was peeled off from the master mold (Figure 1c). In parallel, NOA73 was spin-coated on a glass substrate for 15 s at 500 rpm and then 45s at 3000 rpm (Figure 1d). Subsequently, the spatially modulated UV light was irradiated to the thin film of NOA73 (Figure 1e). Then, the PDMS replica was placed on the partially cured NOA73 thin film to make conformal contact inducing the capillary rise of NOA73 into the cavities (Figure 1f). The shape fixation of NOA73 was performed by applying an additional UV dose for 180 s (30 mW/cm^2). Eventually, the PDMS replica was peeled off from the substrate to release the structure of NOA73 (Figure 1g).

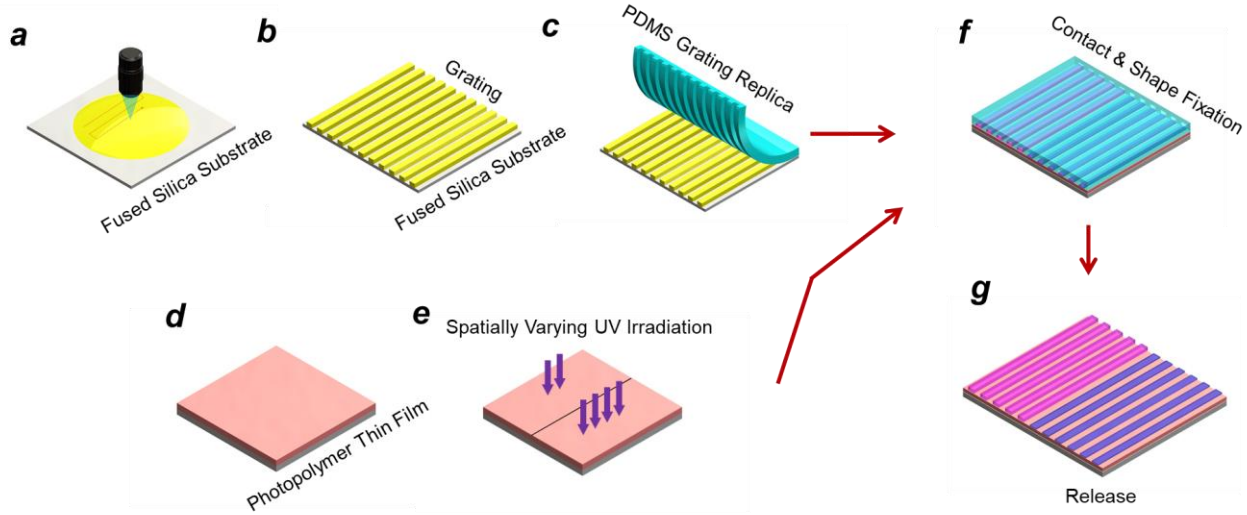

Figure 1. Steps of the light-controlled CFL (a) A fabrication of the master mold using TPL (b) The fabricated master mold (3 μm in pitch, 1.2 μm in height, 1.5 μm in width) (c) Replica molding process to obtain the PDMS nanotextures for CFL (d) A spin-coated photopolymer thin film (e) A spatially varying UV irradiation to the thin film of the photopolymer using SLM (f) Contact and shape fixation by applying additional UV dose for 180 s (30 mW/cm^2) (g) After being completely cured, the finalized structure of NOA73 was released

3. EXPERIMENTAL RESULTS

3.1 Optically height-controlled CFL

Figure 2 shows the result of the light-controlled CFL. Figure 2b-e shows the height of the structure as it was scanned using atomic force microscopy (AFM). As a result, the final height *h* clearly shows the inversely proportional relationship to the given UV dose since the UV premodification decreases the volume of NOA73 that is available for the capillary actions and increases the viscosity of NOA73, both of which impede capillary rise. 10 samples were created for each value of the height in relation to the applied UV dose, and their statistical data were shown in Figure 2a.

In Figure 2b-e, the AFM scans of the structure realized with UV dose of 0, 100, 200, and 300 mJ/cm^2 were plotted for a facile comparison of the height variation. The corresponding height was measured to be 1123 ± 16 nm, 964 ± 8 nm, 843 ± 34 nm, and 121 ± 28 nm, respectively. It obviously exhibits the accuracy and reliability of the light-controlled CFL in relation to the applied UV dose. The light-controlled CFL can accurately adjust the appropriate height for numerous applications based on the collected data.

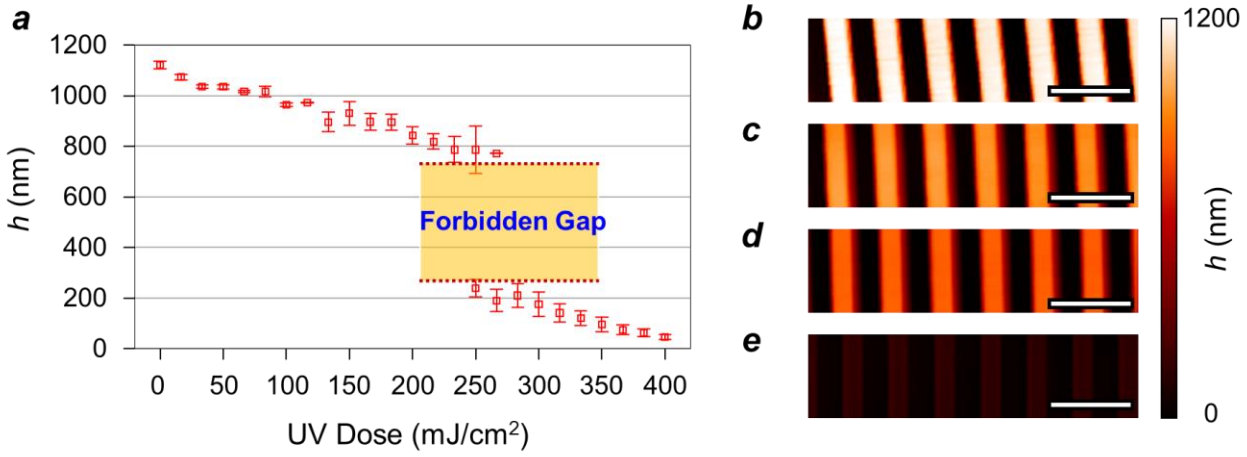

Figure 2. (a) Final height vs. UV dose relation – it clearly shows the inverse proportionality between the final height and the applied UV dose. The error bars indicate standard deviations from 10 measurements. The data shows the unreachable gap between 220 and 800 nm. (b) AFM scans of the NOA73's structure realized with the applied UV dose of 0, (c) 100, (d) 200, and (3) 300 mJ/cm^2 (scale bar: 5 μm)

3.2 Instability of photopolymer's capillarity

The relationship between the applied UV dose and the final height over the entire UV dose range 0 to 400 mJ/cm^2 shown in Figure 2a. The displayed result shows a polymeric capillarity anomaly that the volume-controlled model is unable to account for. The value of *h* surges abruptly at the dosage level of 250 mJ/cm^2, leaving the forbidden gap in the possible *h* value.

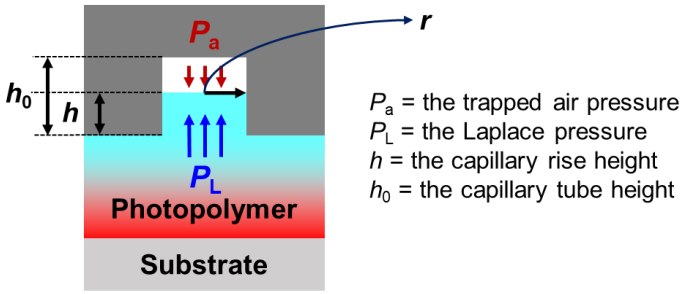

Figure 3. Schematic illustration of the capillary action inside of the cavity.

The forbidden gap can be explained by hypothesizing that the air permeability of the PDMS is low[11]. For the capillary action in the cavity with radius r, as shown in the Figure 3, the Laplace pressure P_L is the main driving force and is given by,

$$P_L = \frac{2}{a}\gamma_{LV}\cos\theta \tag{1}$$

, where γ_{LV} is the surface tension of NOA73, θ is the contact angle between liquid and the wall of the cavity. If the capillary action arises at atmospheric pressure and the capillary risen height is h, the capillary tube height is h_0, then the pressure of the trapped air in the capillary tube P_a can be expressed as,

$$P_a = P_0 \times \frac{h_0}{h_0 - h} \tag{2}$$

, where P_0 is the initial air pressure (1 atm). The capillary action will cease when P_a equals to the P_L. For NOA73 the surface tension is 0.04 N/m in our cavities[12], the calculated Laplace pressure $\Delta P_L \sim 2\gamma_{LV}/r$ is lower than 1.2 atm. In this case, when the capillary risen height h reaches to 200 nm, the capillary rise will cease. The estimated result of onset of the abrupt jump in capillary action are in good agreement with the experimental results ($h \sim 220$ nm). In the lower applied UV dose (< 250 mJ/cm^2), we hypothesized that the organic molecule in the partially cured NOA73 can plasticize the PDMS, rendering PDMS "virtually" air permeable[7]. Accordingly, the capillary risen height h, it rises very rapidly leading to the abrupt jumps above 800 nm in h.

4. APPLICATIONS

The light-controlled CFL is highly capable of patterning with microscale resolutions by applying SLM since the properties of NOA73 rely on the applied UV dose. Figure 4 illustrates how we took advantage of this practical feature to expand the application of the light-controlled CFL into the spatially modulated structure coloring. As the SLM, we adopted a 13.2 μm pitch digital micromirror device (DMD). We firstly illuminated a collimated UV light onto the micromirror array to spatially modulate the reflected incident light. We could precisely adjust the applied UV dose in time using the pre-programmed ON/OFF time sequence with the schematically illustrated desired pattern in Figure 4a.

Figure 4b shows the configuration for examining the colors created by a spatially height-modulated of diffraction gratings. The sample was irradiated with white light at a normal incidence angle, and the optical microscope captured the transmitted light from the sample. The 5x objective lens (numerical aperture (NA) = 0.10) was utilized since the higher magnification and NA is possible to collect the higher order diffracted light.

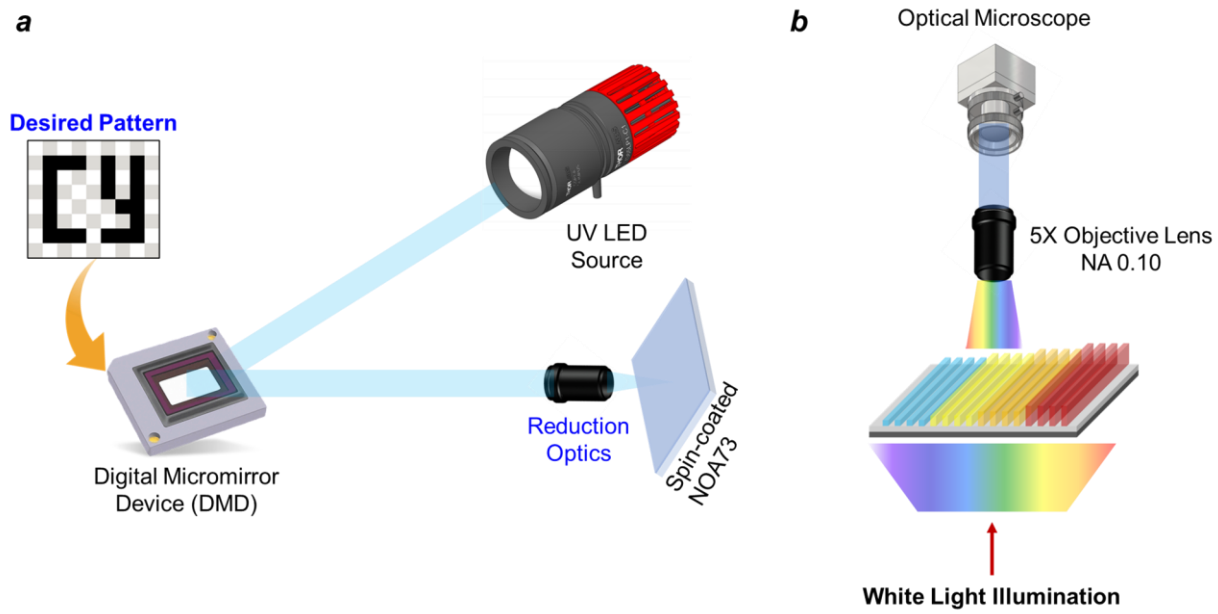

Figure 4. (a) The light controlled CFL with SLM to obtain different height of the structure for microscale resolution patterning. (b) Setup for observing the sample comprises of the spatially modulated height grating. When white light illuminates the sample, the light collected by the optical microscope forms the desired color.

4.1 Structural coloring of the 1D diffraction gratings

Structure color is the creation of color through the interference effects rather than by pigments on the micro- or nanostructured surfaces. Under the normal incidence, structure colors are produced when light passes through a grating owing to the interference of light from the grating and its surroundings (Figure 5a). The height of the grating and the refractive indices of the periodic areas can both affect the intensity of zeroth order diffraction[13]. The intensity of zeroth order diffracted light can be expressed as,

$$I_0 = 1 - 2\frac{W}{\Lambda}\left(1 - \frac{W}{\Lambda}\right) + 2\frac{W}{\Lambda}\left(1 - \frac{W}{\Lambda}\right)cos\left[\frac{2\pi}{\lambda}h(n_1 - n_2)\right] \quad (3)$$

, where W is the width of the grating, Λ is the pitch of the grating, n_1 is the refractive index of NOA73 (1.56), n_2 is the air refractive index (1.00), and λ is the wavelength of incident light, h is the final height of the grating. Equation (3) indicates that the intensity of the zeroth order diffraction is affected by all parameters in the grating. Using the light controlled CFL, we can vary the height h of the grating. Therefore, by varying h, we calculated the peak wavelength λ of the zeroth order with respect to the height. As shown in the Figure 5b, at h = 1200, 1000, and 800 nm, the transmitted peak wavelength λ is 620 (Orange), 560 (Yellow), and 447 (Blue) nm, respectively.

The fabricated grating with the applied UV dose 0, 100, and 200 mJ/cm^2 clearly shows the orange, yellow, and blue at h = 1123 ± 16 nm, 964 ± 8 nm, and 843 ± 34 nm, respectively. Consequently, estimated and experimentally observed colors are in good agreements with each other.

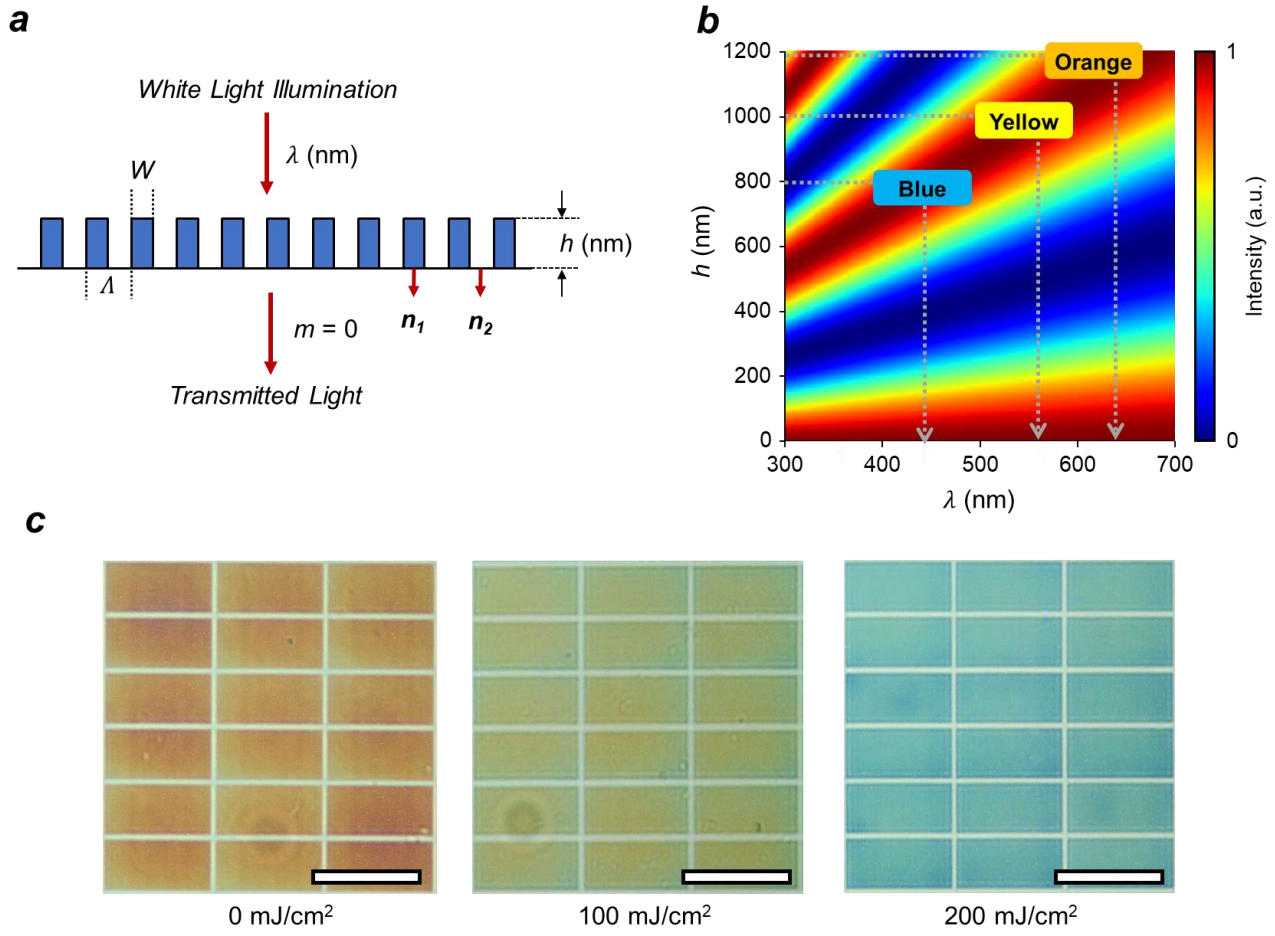

Figure 5. (a) Schematic illustration of the side view of a diffraction grating where W is the width of the grating, Λ is the pitch of the grating, n_1 is the refractive index of NOA73 (1.56), n_2 is the air refractive index (1.00), and λ is the wavelength of incident light, h is the final height of the grating. (b) Simulation on the transmission spectra of the zeroth order with respect to the final height of the NOA73 structure. (c) Optically observed color using optical microscope at h = 1123 ± 16 nm (0 mJ/cm^2), 964 ± 8 nm (100 mJ/cm^2), and 843 ± 34 nm (200 mJ/cm^2), orange, yellow, and blue, respectively (scale bars: 100 μm).

4.2 Microscale patterning with light controlled CFL with SLM

The advantage of the light-controlled CFL is that light can be patterned with SLM at microscale resolutions. The orange, yellow, blue, and transparent color was chosen to generate microscale patterns on the diffraction gratings. The corresponding UV dose for orange, yellow, blue color, and transparent color is 0, 100, 200, and 300 mJ/cm^2, respectively. With these colors, we formed the several combinations with the "C" and "Y" letters and its background.

As shown in Figure 7a and b, we varied the background height while the letters remained unexposed to the UV light. As a result, we obtained the blue and yellow color for the background, and obtained the orange color for the letters. Subsequently, we changed the UV dose for the letters and the background simultaneously. Accordingly, we obtained the different color combination of the letters and the background in Figure 7c-e. In Figure 7f-h, we only changed the UV dose to background. The corresponding results clearly show the changing in the background except the letters. Additionally, orange colored "SPIE PHOTONICS WEST 2023" letters were patterned with different background colors in Figure 8a and b, blue and yellow, respectively.

By utilizing the SLM, UV light was successfully illuminated and pre-modified the NOA73 using pre-programmed ON/OFF sequence resulting in the height variation. The spatial layout can be further varied and tailored for anti-counterfeiting, authentication, and cryptography, as shown in Figures 6 and 7.

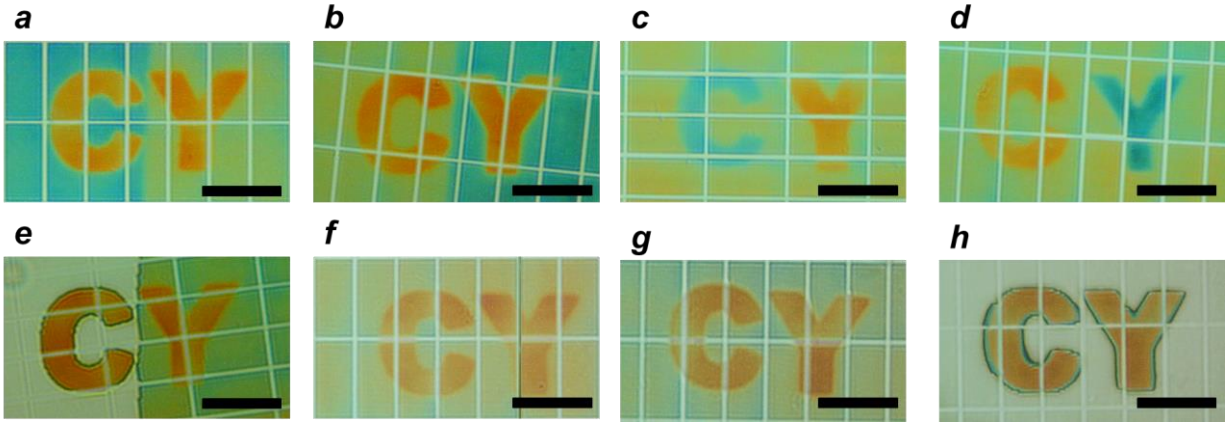

Figure 6. Microscale patterning with light controlled CFL with SLM using "C" and "Y" letters (scale bars: 100 μm) (a) "C" letter in blue background and "Y" letter in yellow background, (b) "C" letter in yellow background and "Y" letter in blue background, (c) Blue colored "C" letter and orange colored "Y" in yellow background, (d) Orange colored "C" letter and blue colored "Y" in yellow background, (e) Orange colored "C" in transparent background and "Y" in yellow background, (f) Orange colored "CY" in yellow background, (g) Orange colored "CY" in blue background, (h) Orange colored "CY" in transparent background.

5. CONCLUSIONS

In conclusion, we have demonstrated light control CFL with SLM for structural coloring. We experimentally controlled the photopolymer's final capillary rise. Accordingly, we noticed very intriguing occurrences, such as the instability of the polymeric capillary rise that caused the formation of the forbidden gap. Also, we found that the "virtual" air permeability of the PDMS causes the abrupt jump in the capillary rise. From these observations and analysis, we can enhance the understanding of the capillary effect.

In addition, we also extended our techniques into the structural coloring applications. Although the light-controlled CFL is required to optimize UV light control and spatial modulation, we predict that this will considerably improve nanoscale manufacturing technology, which can then be used for anti-counterfeiting, authentication, and cryptography. Additionally, it will be providing and broadening on-demand, cost-effective, and reconfigurable nanoscale fabrication scheme.

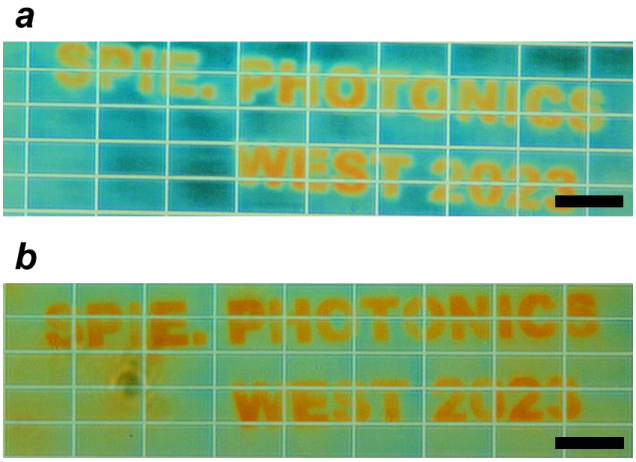

Figure 7. Microscale patterning with light controlled CFL with SLM using "SPIE PHOTONICS WEST 2023" (scale bars: 100 μm) (a) "SPIE PHOTONICS WEST 2023" in blue background, (b) "SPIE PHOTONICS WEST 2023" in yellow background

REFERENCES

[1] Li, Q., Ji, M. G. and Kim, J., "Grayscale Nanopixel Printing at Sub-10-nanometer Vertical Resolution via Light-Controlled Nanocapillarity," ACS Nano 14(5), 6058–6066 (2020).

[2] Li, Q., Ji, M. G., Chapagain, A., Cho, I. H. and Kim, J., "Curvature-Adjustable Polymeric Nanolens Fabrication Using UV-Controlled Nanoimprint Lithography," Micromachines (Basel) 13(12) (2022).

[3] Chan, J. Y. E., Ruan, Q., Wang, H., Wang, H., Liu, H., Yan, Z., Qiu, C. W. and Yang, J. K. W., "Full Geometric Control of Hidden Color Information in Diffraction Gratings under Angled White Light Illumination," Nano Lett 22(20), 8189–8195 (2022).

[4] Lee, Y., Bae, S.-I., Eom, J., Suh, H.-C. and Jeong, K.-H., "Antireflective glass nanoholes on optical lenses," Opt Express 26(11), 14786 (2018).

[5] Siddique, R. H., Gomard, G. and Hölscher, H., "The role of random nanostructures for the omnidirectional anti-reflection properties of the glasswing butterfly," Nat Commun 6, 1–8 (2015).

[6] Gu, Y., Zhang, L., Yang, J. K. W., Yeo, S. P. and Qiu, C. W., "Color generation via subwavelength plasmonic nanostructures," Nanoscale 7(15), 6409–6419 (2015).

[7] Daqiqeh Rezaei, S., Ho, J., Naderi, A., Tavakkoli Yaraki, M., Wang, T., Dong, Z., Ramakrishna, S. and Yang, J. K. W., "Tunable, Cost-Effective, and Scalable Structural Colors for Sensing and Consumer Products," Adv Opt Mater 7(20) (2019).

[8] Stavis, S. M., Strychalski, E. A. and Gaitan, M., "Nanofluidic structures with complex three-dimensional surfaces," Nanotechnology 20(16) (2009).

[9] Jeong, H. E., Kwak, R., Khademhosseini, A. and Suh, K. Y., "UV-assisted capillary force lithography for engineering biomimetic multiscale hierarchical structures: From lotus leaf to gecko foot hairs," Nanoscale 1(3), 331–338 (2009).

[10] Ho, D., Zou, J., Zdyrko, B., Iyer, K. S. and Luzinov, I., "Capillary force lithography: The versatility of this facile approach in developing nanoscale applications," Nanoscale 7(2), 401–414 (2015).

[11] Yoon, H., Kim, T. il, Choi, S., Suh, K. Y., Kim, M. J. and Lee, H. H., "Capillary force lithography with impermeable molds," Appl Phys Lett 88(25) (2006).

[12] Kolliopoulos, P., Jochem, K. S., Lade, R. K., Francis, L. F. and Kumar, S., "Capillary Flow with Evaporation in Open Rectangular Microchannels," Langmuir 35(24), 8131–8143 (2019).

[13] Zhang, D., Men, L. and Chen, Q., "Femtosecond laser fabricated polymeric grating for spectral tuning," J Phys Commun 2(9) (2018).